Brain Stimulation 13 (2020) 1527–1534

Contents lists available at ScienceDirect

Brain Stimulation

journal homepage: http://www.journals.elsevier.com/brain-stimulation

Transcranial ultrasound stimulation in humans is associated with an auditory confound that can be effectively masked

Verena Braun [a], Joseph Blackmore [b], Robin O. Cleveland [b, **], Christopher R. Butler [a, c, d, *]

[a] Nuffield Department of Clinical Neurosciences, University of Oxford, UK
[b] Institute of Biomedical Engineering, University of Oxford, UK
[c] Department of Brain Sciences, Imperial College London, UK
[d] Departamento de Neurología, Pontificia Universidad Católica de Chile, Santiago, Chile

ARTICLE INFO

Article history:
Received 30 January 2020
Received in revised form
24 August 2020
Accepted 27 August 2020
Available online 4 September 2020

Keywords:
Transcranial ultrasound stimulation (TUS)
EEG
Human auditory perception
Neuromodulation
Non-invasive

ABSTRACT

Background: Transcranial ultrasound stimulation (TUS) is emerging as a potentially powerful, non-invasive technique for focal brain stimulation. Recent animal work suggests, however, that TUS effects may be confounded by indirect stimulation of early auditory pathways.
Objective: We aimed to investigate in human participants whether TUS elicits audible sounds and if these can be masked by an audio signal.
Methods: In 18 healthy participants, T1-weighted magnetic resonance brain imaging was acquired for 3D ultrasound simulations to determine optimal transducer placements and source amplitudes. Thermal simulations ensured that temperature rises were <0.5 °C at the target and <3 °C in the skull. To test for non-specific auditory activation, TUS (500 kHz, 300 ms burst, modulated at 1 kHz with 50% duty cycle) was applied to primary visual cortex and participants were asked to distinguish stimulation from non-stimulation trials. EEG was recorded throughout the task. Furthermore, ex-vivo skull experiments tested for the presence of skull vibrations during TUS.
Results: We found that participants can hear sound during TUS and can distinguish between stimulation and non-stimulation trials. This was corroborated by EEG recordings indicating auditory activation associated with TUS. Delivering an audio waveform to participants through earphones while TUS was applied reduced detection rates to chance level and abolished the TUS-induced auditory EEG signal. Ex vivo skull experiments demonstrated that sound is conducted through the skull at the pulse repetition frequency of the ultrasound.
Conclusion: Future studies using TUS in humans need to take this auditory confound into account and mask stimulation appropriately.

Introduction

Transcranial ultrasound stimulation (TUS) uses low intensity focused ultrasound delivered through the skull to cause direct modulation of neuronal function [1–4]. In animal studies, TUS has been shown to modulate activity in several brain areas, including sensorimotor regions, visual cortex, frontal eye fields, anterior cingulate cortex and thalamic targets, resulting in behavioural as well as electrophysiological changes [5–20]. Furthermore, longer term connectivity changes have been identified in non-human primates following offline TUS [4,21]. Several studies have shown that TUS can be applied safely to healthy human participants [22] to modulate behaviour and neural activity in brain regions including somatosensory, visual, and motor cortex as well as to deeper thalamic nuclei [23–28]. These data have resulted in TUS emerging as a safe, potent, non-invasive brain stimulation tool [1], with better spatial accuracy and greater depth than established techniques such as transcranial magnetic or electrical stimulation [29].

However, recent reports from rodent studies have suggested that behavioural and neural effects of TUS may in fact result from

Abbreviations: BDC, burst duty cycle; EEG, electroencephalography; ERP, event related potential; IQR, interquartile range; PRF, pulse repetition frequency; TUS, transcranial ultrasound stimulation.

* Corresponding author. Department of Brain Sciences, Imperial College London, UK
** Corresponding author.
E-mail addresses: robin.cleveland@eng.ox.ac.uk (R.O. Cleveland), christopher.butler@imperial.ac.uk (C.R. Butler).

https://doi.org/10.1016/j.brs.2020.08.014

indirect widespread auditory activation [30,31]. In guinea pigs, strong responses in the primary auditory cortex were observed independent of the sonicated brain target and transection of the auditory nerve or removal of the cochlear fluid abolished the response [30]. In transgenic mice, activity produced by ultrasound bursts strongly resembled activity associated with audible sound and was eliminated by chemical deafening [31]. It has been shown in mice that auditory activation arises from sharp edges in a TUS rectangular envelope stimulus [32] and that the auditory activation could be eliminated by smoothing the onset and offset of a continuous wave stimulation over 12 ms. However, such long smoothing cannot be employed for the 0.5 ms pulses that are commonly used in TUS.

In neurostimulation research it is well accepted that confounding factors have to be carefully controlled [33] in order to ensure that the effects observed are indeed the result of having stimulated a certain brain area, rather than by extraneous effects such as somatosensory stimulation [34,35]. In TUS this is particularly important since the precise mechanisms by which neuromodulation occurs are not well understood, although these remain the subject of intense research efforts [36]. It is important therefore to determine whether TUS may also have auditory side-effects in humans that could impact outcomes.

Using stimulation parameters similar to those employed in previous human studies, we applied TUS for 300 ms at 500 kHz modulated with a 1 kHz square wave (50% burst duty cycle (BDC)) to the right visual cortex of 18 healthy human participants. Stimulation and sham trials were presented in randomised order and subjects were asked to distinguish trials with active stimulation from trials in which no stimulation was applied. EEG was recorded throughout. Participants were reliably able to hear sound during stimulation trials, and therefore we further investigated the nature of this phenomenon with ex vivo skull recordings and tested the behavioural and electrophysiological effectiveness of auditory stimulus masking.

Material and methods

TUS-EEG

Participants

Participants were screened for contraindications against brain stimulation [37] and magnetic resonance imaging and did not report hearing impairments. They were part of a larger study looking into the effects of TUS on visual processing and were remunerated for their time. This manuscript reports data from 18 healthy human participants who completed this part of the study (11 female and 7 male, mean age 26.22± 7.25 years). Informed consent was acquired from every participant prior to the experiment. The study was approved by the University of Oxford Medical Sciences Interdivisional Research Ethics Committee.

Experimental setup and procedure

The experiment was split into two blocks (Fig. 1a and b) which were conducted in the same order by every participant. First, participants took part in the unmasked block. This part consisted of 100 trials (50 stimulation, 50 sham stimulation trials) which were presented in randomised order. Participants were asked to keep their eyes fixed at the centre of a computer screen. In stimulation trials, TUS was applied 2.7–3 s after fixation onset for 300 ms before a question mark appeared prompting participants to indicate whether they thought they were stimulated or not, using their right hand. This block was followed by the masked block in which a masking tone was played through earphones in every trial, approximately 112 ms prior to the onset of the ultrasound stimulation for 700 ms, before the question mark appeared prompting participants to indicate whether they thought they were stimulated or not. Similar to the unmasked condition, 100 trials split into 50 stimulation and 50 no stimulation sham trials were presented in randomised order. At the end of each experimental condition block, participants were asked whether they had experienced any positive visual phenomena (such as phosphenes).

Prior to the main experiment, T1-weighted high-resolution images were acquired from every participant with a Siemens 3 T Trio system. For TUS modelling, tissue types were segmented using MARS [38] for SPM 8 (Wellcome Department of Cognitive Neurology, London. UK; www.fil.ion.ucl.ac.uk/spm) and target brain sites were identified visually in the right visual cortex (Fig. 1d).

Both acoustic and thermal participant-specific modelling was carried out to determine appropriate source locations and amplitudes in order to focus to the intended targets as well as satisfy the safety constraints (maximum peak modelled pressure in CSF or brain tissue = 0.6 MPa, maximum temperature rise in skull bone = 3 °C, maximum temperature rise in brain tissue = 1 °C) similar to other studies involving human subjects (see Fig. 2 of Ref [36]). Numerical modelling was carried out using k-Wave, a pseudospectral time domain solver [39]. For the acoustic simulations, the skull bone was treated as a homogeneous medium and an effective fluid with transducer positions and orientations selected based on the phase distributions obtained from back-propagation of an US source positioned at the target to the source. Subsequent forwards simulations were then conducted to determine the in situ pressure fields and amplitudes, and hence determine appropriate source intensities. Finally, thermal simulations were carried out to calculate the associated temperature rises based on the estimated pressure fields. More details on the modelling protocol can be found in Blackmore et al. [40].

Ultrasound stimulation was delivered through a 500 kHz single-element geometrically-focused (64 mm aperture, 63.1 mm radius of curvature) transducer (H-107, Sonic Concepts Inc, Bothell, WA, USA). One stimulation trial consisted of a 300 ms burst applied at a 1 kHz pulse repetition frequency (PRF) and 50% BDC as shown in Fig. 1a and b. The waveform was produced by an arbitrary waveform generator (Handyscope HS5, TiePie, WL Sneek, The Netherlands), amplified by a 55 dB broadband amplifier (1140LA, E&I, Rochester, NY, USA), and connected to the transducer via a matching network. The arbitrary waveform generator also generated a timing pulse which was recorded by the EEG to ensure synchronisation of ultrasound and EEG signals.

The ultrasound transducer was coupled to the scalp using a flexible polyurethane membrane (see Fig. 3a). This was fixed around the edges of the transducer using a custom mount with an o-ring seal. The cone was filled with degassed water through syringe connections on a back plate over the central circular transducer cut-out. Ultrasound coupling gel was liberally applied to the scalp of the subject before the coupling membrane was applied. The placement of the transducer was guided by a neuronavigation system (Brainsight; Rogue Resolutions; https://www.rogue-resolutions.com) with optical trackers placed on both the transducer and the subject.

EEG recording and preprocessing

EEG was recorded throughout the task from 54 Ag/AgCl sintered ring electrodes (BrainProducts 64-channel BrainAmp DC, BrainProducts GmbH, Gilching, Germany) arranged according to the 10%-system at a sampling rate of 500 Hz (low cutoff 10 s, high cutoff 250 Hz) referenced to FCz. EEG data were preprocessed and analysed using Fieldtrip [41] as well as in-house MATLAB scripts. EEG data were first epoched −1 s–1.5 s around stimulation onset and

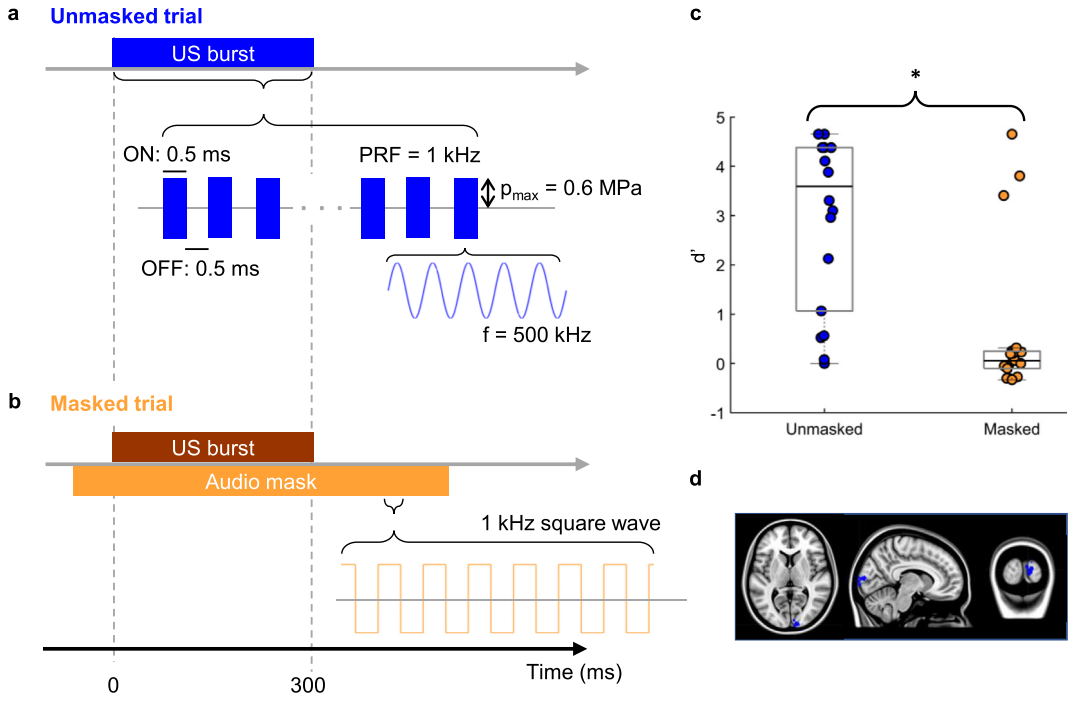

Fig. 1. Experimental design and results. Participants performed a detection task in which they were asked to indicate whether a given trial was a stimulation or sham trial. The experiment was split into two conditions and was always administered in the same order starting with unmasked trials. **a, Unmasked trials.** In the unmasked condition, participants received TUS in half of the trials, while in the other half no TUS was applied. Each TUS trial consisted of a 300 ms burst, which was made up of 0.5 ms pulses of 500 kHz ultrasound (250 cycles) alternating with 0.5 ms of no ultrasound (that is, a burst duty cycle (BDC) of 50% and PRF of 1 kHz). The maximum modelled peak positive pressure at the target cortical site (V1) was 0.6 MPa **b, Masked trials.** The masked condition comprised the same TUS stimulation protocol but with the addition of an audio mask delivered via earphones to the participants. The audio mask was applied during TUS and sham trials in the masked condition only. The audio mask consisted of a 1 kHz square wave starting approximately 110 ms before TUS onset and lasting 700 ms. **c, Behavioural results.** Boxplots depicting d' values for unmasked and masked trials. Black lines indicate the median d' value and filled circles correspond to individual data points. Detection rates were significantly lower in the masked condition compared to the unmasked condition. Three participants continued to detect stimulation in the presence of the masking signal. **d, Stimulation sites.** Stimulation sites shown in MNI space. Target brain sites were identified visually. Sites were chosen in the right visual cortex that could be reached easily with TUS.

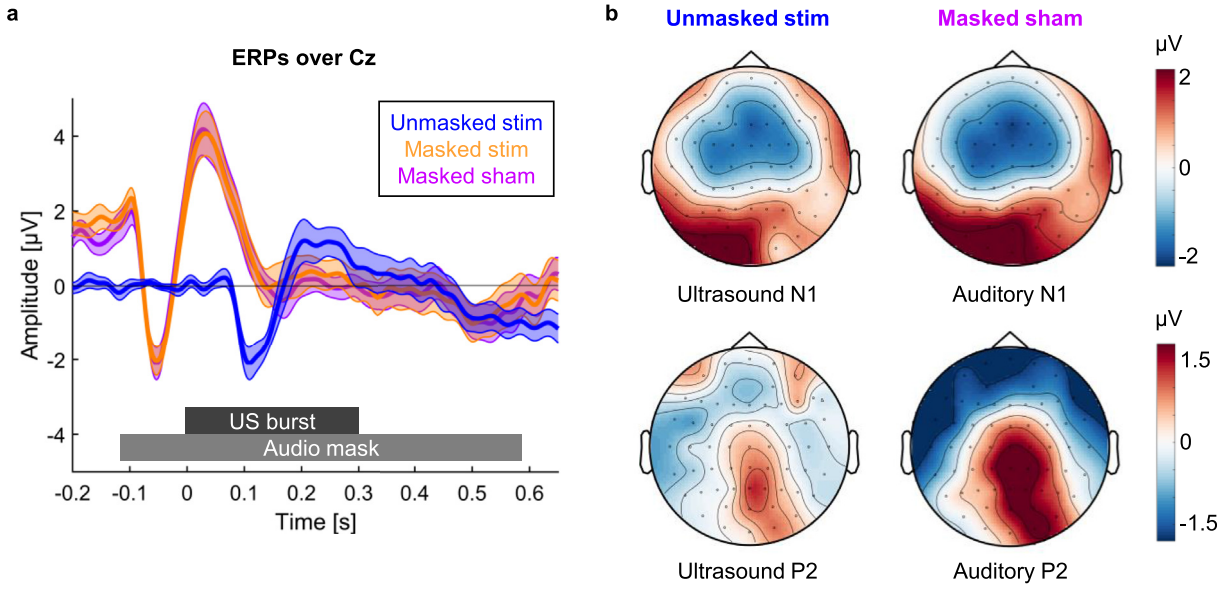

Fig. 2. ERP results. a, ERP waveforms over Cz. ERPs over Cz for stimulation trials in the unmasked (blue) and masked (orange) condition as well as sham trials in the masked condition (purple) are shown. The unmasked ERP shows a response 100 ms after stimulation confirming that TUS induces an auditory ERP. The masked ERP shows a response to the masking audio tone starting 100 ms before the onset of the TUS burst. Shaded area represents standard error of the mean. **b, Comparison of ultrasound ERPs and auditory ERPs**. US-N1 amplitude was defined as the mean amplitude 50–150 ms after stimulation onset, whereas US-P2 amplitude was defined as the mean amplitude 150–250 ms after stimulation onset (baseline window: 0.1 s–0 s). Auditory N1 amplitude was defined as the mean amplitude −100 to 0 ms before stimulation onset, whereas the auditory P2 component was extracted by taking the mean amplitude 0–100 ms after stimulation onset (baseline window: 0.21 s to −0.11 s). (For interpretation of the references to colour in this figure legend, the reader is referred to the Web version of this article.)

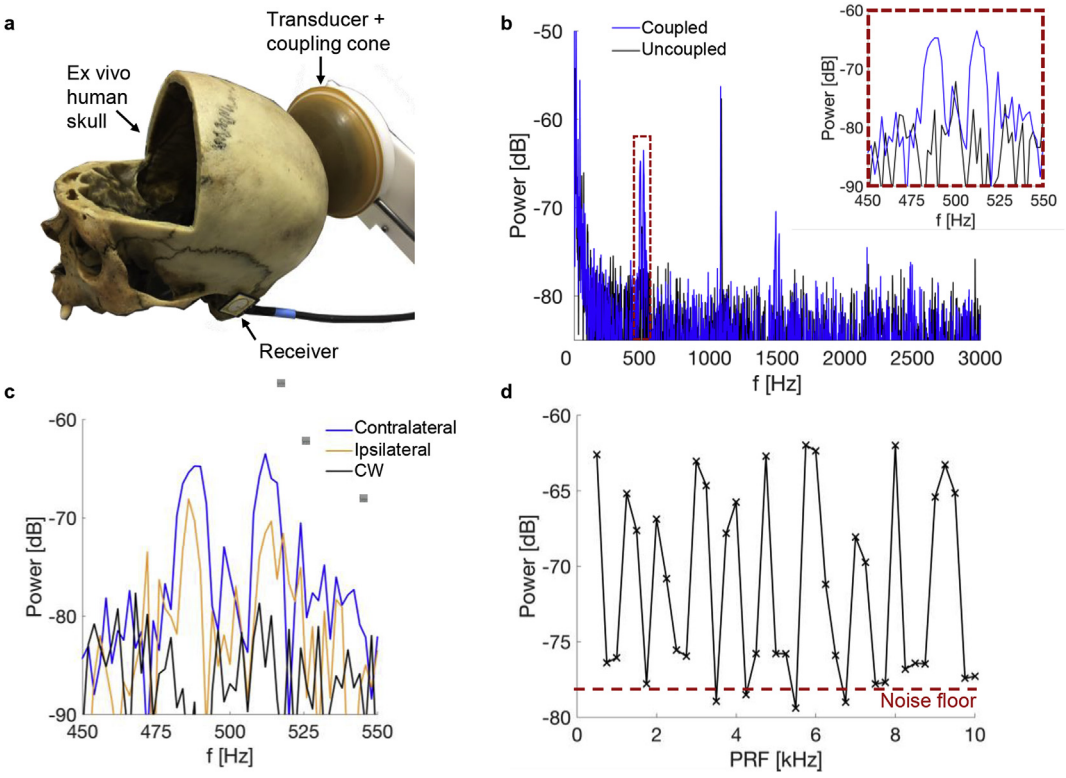

Fig. 3. Vibration detection in an ex vivo human skull. a, Experimental setup: the TUS transducer was coupled posteriorly to an ex vivo human skull (the frontal skull portion had been removed for other purposes) via an expandable, water-filled coupling cone and US coupling gel. Vibrations were detected using a broadband receiver (700 Hz–20 kHz) placed near the ear contralateral to the transducer. **b**, Power spectra for the received waveform with the receiver coupled and uncoupled to the skull. The applied US waveform was a 300 ms burst at a 50% duty cycle and 500 Hz PRF. Note that the signal identified at ~1 kHz was a stray electromagnetic signal in the laboratory present whether the transducer was coupled or not. **c**, Recorded power spectra with the receiver positioned either contralateral or ipsilateral with respect to the transducer and for a continuous wave 300 ms US pulse. **d**, Power spectra amplitudes as a function of PRF. The maximum power in a 40 Hz window around the nominal PRF was extracted as the PRF was increased from 500 Hz to 10 kHz in steps of 250 Hz. The amplitude of the noise floor is indicated by the red dashed line. (For interpretation of the references to colour in this figure legend, the reader is referred to the Web version of this article.)

visually inspected for artefacts. In order to identify ocular and muscle artefacts an independent components analysis was applied before the cleaned data were again visually inspected and trials containing remaining artefacts removed. Channels that had to be removed in order to allow room for the transducer to be coupled were subsequently reconstructed using a weighted neighbour approach as implemented in the fieldtrip toolbox [41] before re-referencing the data to common average reference, resulting in 60 electrodes in total.

Data analysis

Behaviour. Behavioural data were analysed using in-house MATLAB scripts and JASP (JASP Team (2019). JASP(Version 0.9.2) [Computer software]). In order to assess participants' ability to distinguish stimulation from sham trials, *d'* values were calculated by subtracting normalised false alarm rates from normalised hit rates. A hit was defined as a stimulation trial that was correctly identified as such, whereas a sham trial that was falsely identified as an active stimulation trial was classified as a false alarm. Since *d'* values for masked and unmasked trials deviated from normality (Shapiro-Wilk Test: unmasked: $W = 0.830$, $p = 0.004$; masked: $W = 0.603$, $p < 0.001$), one sample Wilcoxon signed-rank tests were conducted. Matched rank biserial correlations are reported as effect sizes for the Wilcoxon test. Masking success was further determined by conducting dependent samples t-tests comparing *d'* values in the unmasked and masked condition. Effect sizes were estimated using Cohen's d. Outliers were identified as values higher than Q3 + 1.5 times the interquartile range.

EEG. To investigate stimulation evoked effects, data were low-pass filtered at 30 Hz and event related potentials (ERPs) were computed for every participant (baseline: -100 ms–0 ms). In order to assess auditory activity associated with TUS, event-related potentials over EEG electrode Cz were extracted [42–44] and two main components analysed. US-P2 amplitude was defined as the mean amplitude 150–250 ms after stimulation onset while US-N1 amplitude as the mean amplitude 50–150 ms after stimulation onset. Mean US-P2 and US-N1 amplitudes were compared between conditions using repeated measures ANOVAs and follow-up dependent samples t-tests. Effect sizes for ANOVAs were estimated using partial eta squared (η^2_p), whereas Cohen's d was used to estimated effect sizes for post-hoc t-tests.

Skull audio recordings

Given the previously cited work in rodents [30,31], we hypothesised that auditory activation may be due to bone conduction: that is, as TUS passes through the skull it induces a radiation force on the skull at the modulation frequency which then propagates through the skull as a flexural wave to the cochlea, stimulating the standard acoustic pathway [45]. The possible coupling to flexural waves was investigated using an ex vivo human skull in air. In this instance, the ultrasound transducer was coupled to the skull with the coupling cone and US gel and a piezoelectric transducer (SPS-2220-03, Sonitron, Sint-Niklass, Belgium), with an active area 16 mm × 20 mm and bandwidth of 700 Hz to 20 kHz, was coupled to the skull close to the ear canal (see Fig. 3a). All

incident US bursts were 300 ms in length at a 50% BDC and a PRF that was varied from 250 Hz to 10 kHz in steps of 250 Hz.

Results

Behaviour

D′ results for unmasked and masked trials are shown in Fig. 1c. Without auditory masking, most participants were reliably able to detect stimulation trials ($V = 153$, $p < 0.001$, rank-biserial correlation = 0.789). 16 participants described being able, on some trials, to hear a high-pitched tone and associated this with stimulation. The other two participants reported hearing no such sound and performed very close to chance level on the detection task. Masking the stimulation-induced sound with a masking tone resulted in detection rates not significantly different from zero ($V = 98$, $p = 0.320$, rank-biserial correlation = 0.146). Masking success was further assessed by comparing *d'* values between the two conditions directly. A dependent samples *t*-test revealed a significant reduction in *d'* values when masking was applied ($t(17) = 4.352$, $p < 0.001$, Cohen's $d = 1.026$, 95% CI for the mean difference = [1.170 3.372]). Although the overall group *d'* did not significantly differ from zero when masking was applied, three participants were still able to detect the stimulation with *d'* values of 4.653, 3.804, and 3.407 (Fig. 1c). These three outliers described the stimulation trials as being signalled by an additional, slightly higher pitched tone during the longer audio masking sound, although it was a subtle difference only evident when specifically listening for it. Only one participant of all 18 reported having seen phosphenes – described as 'intermittent black ripples' visualised over the lower left quadrant of the computer screen – and reported having seen these during both the unmasked and masked blocks. Numerical modelling for this participant showed the pressure at the V1 target to be 0.59 MPa, in the upper quartile but not at the top of the range (group mean = 0.50 MPa, SD = 0.08, range 0.30–0.60). This participant was not one of the three outliers able reliably to detect stimulation during the masked block.

EEG

In order to determine the electrophysiological correlates of effective auditory masking, EEG analyses focused on the 15 participants who were unable to discriminate between stimulation and sham trials in the masked condition. ERP waveforms over Cz are shown in Fig. 2a. In the unmasked condition, stimulation elicited a waveform characteristic of an auditory evoked potential (Fig. 2) [42–44] with a pronounced negative deflection around 100 ms (US-N1: one-sample *t*-test: $t(14) = -5.886$, $p = <0.001$, Cohen's $d = -1.520$, mean = −1.053, 95% CI = [-1.436 -0.669]; US-P2: one-sample *t*-test: $t(14) = 1.360$, $p = 0.195$, Cohen's $d = 0.351$, mean = 0.670, 95% CI = [-0.386 1.726]). This response was abolished when auditory masking was applied. Instead, the ERP was dominated by an earlier and more pronounced auditory evoked potential corresponding to the masking tone. A 2 × 2 repeated-measures ANOVA with the factors MASKING (unmasked vs. masked) and COMPONENT (US-P2, US-N1) revealed a significant MASKING × COMPONENT interaction ($F(1,14) = 15.753$, $p = 0.001$, $\eta^2_p = 0.529$). Post-hoc dependent-samples t-tests revealed that masking significantly affected US-N1 amplitude ($t(14) = -5.279$, $p < 0.001$, Cohen's $d = -1.363$, mean difference = −2.518, 95% CI = [-3.541 -1.495] while no difference in US-P2 amplitudes could be observed ($t(14) = 0.560$, $p = 0.584$, Cohen's $d = 0.145$, mean difference = 0.423, 95% CI = [-1.196 2.041]).

In order to test whether any differences between stimulation and sham during masking can be observed, we conducted an additional 2 × 2 repeated-measures ANOVA with the factors STIMULATION CONDITION (stimulation vs. sham) and COMPONENT (US-P2, US-N1). This analysis only revealed a significant main effect of the factor COMPONENT ($F(1,14) = 9.816$, $p = 0.007$, $\eta^2_p = 0.412$. No differences between stimulation and sham could be found (STIMULATION CONDITION x COMPONENT: $F(1,14) = 3.253$, $p = 0.093$, $\eta^2_p = 0.189$).

Ex vivo skull recording

The experimental setup we used to investigate our hypothesis that auditory activation was due to bone conduction is shown in Fig. 3a. The modulation frequency was varied from 250 Hz to 10 kHz and Fig. 3b shows the Fourier transform of signals recorded by the piezoelectric receiver for a 500 Hz modulation. The presence of peaks at the modulation frequency of 500 Hz, and the odd harmonics at 1500 Hz and 2500 Hz, are consistent with the hypothesis that the 500 kHz ultrasound signal is being absorbed and producing skull vibrations due to the square wave modulation, which is in the audible range. When the receiver was uncoupled, the peaks were not present, indicating that the signal was not airborne. Note that the signal identified at around 1 kHz was a stray electromagnetic signal in the laboratory that was present whether the transducer was coupled or not. Interestingly, the spectra at each of the frequencies were split into two peaks approximately 10 Hz either side of the nominal frequency, see inset of Fig. 3 (b). The underlying explanation for this phenomenon is unknown. In particular, there was no 10 Hz modulation present in the signals.

Fig. 3c displays the recorded power spectra±50 Hz around the modulation frequency. To investigate whether peak amplitudes vary as a function of recording site, we compared amplitudes recorded from the contralateral ear canal to the power spectra of recordings at the ear canal ipsilateral to the transducer. This revealed amplitude variations of up to 6 dB, suggesting that skull topology may be important in the transmission of the flexural wave to the ear canals and may result in different sound localisations between participants. Moreover, the signal was not present for 300 ms continuous wave pulses confirming that the recorded waveform is a consequence of the modulating envelope (PRF). Fig. 3d shows the impact of the PRF on the amplitude of the received signals at each corresponding nominal frequency. For each burst, the PRF was increased by 250 Hz up to 10 kHz with the individual pulse lengths adjusted to maintain a BDC of 50%. As in each case the spectrum was again split into two peaks, the maximum amplitude in a 40 Hz window around the driving PRF was extracted. The peak amplitude rose up to 15 dB above the noise floor but at some frequencies disappeared into the noise, suggesting that the strength of the frequency response may be dependent on the modulation frequency as well as individual skull structure. This could contribute to differences between subjects in their ability to detect the acoustic confound and is discussed below.

Discussion

TUS is seen as the newest addition to a collection of methods that non-invasively stimulate the brain in order to investigate causal relationships between brain function and behaviour [1]. We investigated whether TUS can feasibly be applied to healthy human participants without the need for additional sham stimulation conditions. Eighteen healthy human participants received TUS to the visual cortex randomly intermixed with trials without stimulation. While only one subject reported having seen phosphenes during stimulation, we found reliable electrophysiological and behavioural evidence of auditory activation during TUS. Participants reported hearing an audible tone that enabled them to

distinguish between stimulation and non-stimulation trials, and ERP waveforms time-locked to stimulation onset resembled activity elicited by audible sound. Our findings indicate that sham stimulation conditions need to be adjusted to control for these unwanted auditory effects. We note that the rarity of phosphene detection in our experiment, when compared to the results of Lee et al. [26], may be attributable to a range of differences in experimental protocol. In particular, in contrast to Lee et al., we did not reduce ambient light nor ask participants to close their eyes and concentrate specifically on phosphenes, but rather to report, on each trial, whether they thought they had received ultrasound stimulation or not. We also used a different US frequency (500 kHz vs 270 kHz) and PRF (1 kHz vs 500 Hz), and interleaved stimulation/no stimulation trials rather than blocking them.

Auditory confounds during TUS have recently been reported in rodents with TUS eliciting nonspecific auditory activation that drives outcome while chemical deafening or transection of the auditory nerve abolished behavioural and cortical responses to TUS [30,31]. However, the exact mechanism behind these effects remains unclear. Gavrilov & Tsirulnikov [46] reviewed evidence from studies conducted in the 1970's also indicating that human participants can perceive a sound during TUS that matches in pitch the frequency of the modulating envelope. In the present study, we also found evidence that modulation of the ultrasound signal may be responsible for the auditory confounds observed. In ex vivo skull recordings we could show that signals at the PRF and its harmonics can be received from the skull. These effects were not present when the receiver was removed from the skull. Our results suggest that it is coupling of the TUS into a physical wave, rather than direct neurostimulation, that results in audible sound.

Carefully constructing control conditions is vital in order to be able to draw causal conclusions about the role the manipulated brain process plays in behavioural outcomes. Controlling for nonspecific side effects of stimulation ensures that any effects observed can be attributed to the manipulation. Sham stimulation conditions have traditionally been tailored to the specific shortcomings of the technique used [34,35]. With TMS, an audible click emitted by the coil can confound both behavioural and electrophysiological responses. A variety of methods has been applied to try and mask this sound including the use of earplugs, white noise or adapted noise played via headphones or earphones, and insertion of a thin layer of foam between the TMS coil and the scalp [51]. In TUS however, so far, most studies compared its effects on behaviour or neural processing to conditions in which stimulation was not applied [26–28], the transducer was tilted away from the head [24,25] or a disc with high acoustic impedance was placed between the transducer and the subject's head [23]. These sham procedures would not induce the acoustic artefact reported here and are therefore not well suited to control for acoustic effects resulting from coupling through the skull. The present study, together with recent animal work [30,31], puts this practice into a new perspective. For TUS to be an effective tool to investigate the causal relationship between brain processes and behaviour, suitable sham stimulation conditions controlling for auditory effects have to be identified.

Our results show that simply not stimulating might not be the most optimal control condition and that future studies using this increasingly popular technique in humans need to take steps to control for auditory confounds. We blinded participants to the stimulation by delivering a masking sound at the PRF. While this was effective in most of our subjects and significantly reduced detection rates, three participants out of 18 could nonetheless tell the difference between active stimulation and sham. This may be the result of individual differences in resonance properties of the skull. Our ex vivo skull recordings revealed a strong frequency response during TUS which is likely skull (participant) and location specific as has been reported in the bone conduction literature [45]. Moreover, varying the PRF revealed that the amplitudes vary substantially at different frequencies. This variation is consistent with experiments on the frequency dependence of bone conduction on cadaveric heads [47]. We note that the use of an air-filled skull means the flexural wave speed will be different than for the case of the skull loaded by soft-tissue, which will alter the locations of the peaks. The result implies that adjustment of the PRF may change the amplitude of the induced wave, possibly dependent on the resonant modes of the skull structure [48]. Masking levels will therefore be subject specific. Further research, in larger groups of participants, is needed to determine the precise interactions between subject-specific variables and experimental parameters that determine individual differences in detection thresholds. In the meantime, for pragmatic purposes, combined adjustment of masking level and PRF may be necessary to minimise detection in experiments using TUS for behavioural modulation. This could be envisaged as a preliminary test before the start of the behavioural experiments, optimising the US waveform for each participant in order to reduce the impact of non-specific auditory activation.

Whether auditory masking is the most effective means to control for auditory confounds or whether control stimulation sites, or other sham conditions, would be more appropriate remains a task for future research. For quasi-continuous wave ultrasound waveforms, it has been shown that smoothing the leading and trailing edges of the pulse can be used to avoid auditory confounds in mice [32], and smoothed waveforms have been used successfully in macaques to modulate neuronal activity [49]. The approach in Ref. [49] employed a 12 ms rise time and fall time to smooth the transients of a quasi-continuous wave insonation, which is possible when the pulse has a duration much longer than the smoothing. However for the 1 kHz PRF employed here, a 12 ms smoothing would attenuate the 0.5 ms long pulses and thus is not an effective approach to mitigate the acoustic confound. The masking employed here was narrowband, consistent with the critical band concept in auditory masking [50], where signals at different frequencies are not as effective at masking tones.

In conclusion, TUS has the potential to be a powerful, non-invasive brain stimulation technique, particularly given its advantages in terms of spatial accuracy and ability to target deep structures. However, auditory confounds should not be neglected and the results reported here provide further evidence for the need to optimise both sham and stimulation parameters.

CRediT authorship contribution statement

Verena Braun: Conceptualization, Data curation, Formal analysis, Investigation, Methodology, Project administration, Visualization, Writing - original draft, Writing - review & editing. **Joseph Blackmore:** Conceptualization, Data curation, Formal analysis, Investigation, Methodology, Project administration, Visualization, Writing - original draft, Writing - review & editing. **Robin O. Cleveland:** Conceptualization, Funding acquisition, Investigation, Methodology, Project administration, Resources, Supervision, Writing - review & editing. **Christopher R. Butler:** Conceptualization, Funding acquisition, Investigation, Methodology, Project administration, Resources, Supervision, Writing - review & editing.

Declaration of competing interest

The authors declare no conflicts of interest.

Acknowledgments

This research was supported by the Medical Research Council [Clinical Scientist Fellowship MR/K010395/1 to C.R.B.)] and the John Fell fund [Grant number 163/11] awarded to C.R.B. J.B. was funded by an EPSRC studentship [EP/F500394/1].

Appendix A. Supplementary data

Supplementary data to this article can be found online at https://doi.org/10.1016/j.brs.2020.08.014.

References

[1] Fomenko A, Neudorfer C, Dallapiazza RF, Kalia SK, Lozano AM. Low-intensity ultrasound neuromodulation: an overview of mechanisms and emerging human applications. Brain Stimul 2018;11:1209–17. https://doi.org/10.1016/j.brs.2018.08.013.
[2] Tufail Y, Matyushov A, Baldwin N, Tauchmann ML, Georges J, Yoshihiro A, et al. Transcranial pulsed ultrasound stimulates intact brain circuits. Neuron 2010;66:681–94. https://doi.org/10.1016/j.neuron.2010.05.008.
[3] Tyler WJ, Tufail Y, Finsterwald M, Tauchmann ML, Olson EJ, Majestic C. Remote excitation of neuronal circuits using low-intensity, low-frequency ultrasound. PLoS One 2008;3:e3511. https://doi.org/10.1371/journal.pone.0003511.
[4] Verhagen L, Gallea C, Folloni D, Constans C, Jensen DEA, Ahnine H, et al. Offline impact of transcranial focused ultrasound on cortical activation in primates. eLife 2019;8:e40541. https://doi.org/10.7554/eLife.40541.
[5] Gulick DW, Li T, Kleim JA, Towe BC. Comparison of electrical and ultrasound neurostimulation in rat motor cortex. Ultrasound MedBiol 2017;43:2824–33. https://doi.org/10.1016/j.ultrasmedbio.2017.08.937.
[6] Han S, Kim M, Kim H, Shin H, Youn I. Ketamine inhibits ultrasound stimulation-induced neuromodulation by blocking cortical neuron activity. Ultrasound MedBiol 2018;44:635–46. https://doi.org/10.1016/j.ultrasmedbio.2017.11.008.
[7] Kamimura HAS, Wang S, Chen H, Wang Q, Aurup C, Acosta C, et al. Focused ultrasound neuromodulation of cortical and subcortical brain structures using 1.9MHz. Med Phys 2016;43:5730–5. https://doi.org/10.1118/1.4963208.
[8] Kim H, Chiu A, Lee SD, Fischer K, Yoo SS. Focused ultrasound-mediated non-invasive brain stimulation: examination of sonication parameters. Brain Stimul 2014;7:748–56. https://doi.org/10.1016/j.brs.2014.06.011.
[9] Kim H, Park HY, Lee SD, Lee W, Chiu A, Yoo SS. Suppression of EEG visual-evoked potentials in rats through neuromodulatory focused ultrasound. Neuroreport 2015;26:211–5. https://doi.org/10.1097/WNR.0000000000000330.
[10] King RL, Brown JR, Newsome WT, Pauly KB. Effective parameters for ultrasound-induced in vivo neurostimulation. Ultrasound MedBiol 2013;39:312–31. https://doi.org/10.1016/j.ultrasmedbio.2012.09.009.
[11] King RL, Brown JR, Pauly KB. Localization of ultrasound-induced *in vivo* neurostimulation in the mouse model. Ultrasound MedBiol 2014;40:1512–22. https://doi.org/10.1016/j.ultrasmedbio.2014.01.020.
[12] Li GF, Zhao HX, Zhou H, Yan F, Wang JY, Xu CX, et al. Improved anatomical specificity of non-invasive neuro-stimulation by high frequency (5 MHz) ultrasound. Sci Rep 2016;6:24738. https://doi.org/10.1038/srep24738.
[13] Mehić E, Xu JM, Caler CJ, Coulson NK, Moritz CT, Mourad PD. Increased anatomical specificity of neuromodulation via modulated focused ultrasound. PLoS One 2014;9:e86939. https://doi.org/10.1371/journal.pone.0086939.
[14] Ye PP, Brown JR, Pauly KB. Frequency dependence of ultrasound neurostimulation in the mouse brain. Ultrasound Med Biol 2016;42:1512–30. https://doi.org/10.1016/j.ultrasmedbio.2016.02.012.
[15] Yoo SS, Bystritsky A, Lee JH, Zhang Y, Fischer K, Min BK, et al. Focused ultrasound modulates region-specific brain activity. Neuroimage 2011;56:1267–75. https://doi.org/10.1016/j.neuroimage.2011.02.058.
[16] Yoo SS, Kim H, Min BK, Franck E, Park S. Transcranial focused ultrasound to the thalamus alters anesthesia time in rats. Neuroreport 2011;22:783–7. https://doi.org/10.1097/WNR.0b013e32834b2957.
[17] Lee W, Lee SD, Park MY, Foley L, Purcell-Estabrook E, Kim H, et al. Image-guided focused ultrasound-mediated regional brain stimulation in sheep. Ultrasound Med Biol 2016;42:459–70. https://doi.org/10.1016/j.ultrasmedbio.2015.10.001.
[18] Dallapiazza RF, Timbie KF, Holmberg S, Gatesman J, Lopes MB, Price RJ, et al. Noninvasive neuromodulation and thalamic mapping with low-intensity focused ultrasound. J Neurosurg 2018;128:875–84. https://doi.org/10.3171/2016.11.JNS16976.
[19] Deffieux T, Younan Y, Wattiez N, Tanter M, Pouget P, Aubry JF. Low-intensity focused ultrasound modulates monkey visuomotor behavior. Curr Biol 2013;23:2430–3. https://doi.org/10.1016/j.cub.2013.10.029.
[20] Fouragnan EF, Chau BKH, Folloni D, Kolling N, Verhagen L, Klein-Flügge M, et al. The macaque anterior cingulate cortex translates counterfactual choice value into actual behavioral change. Nat Neurosci 2019;22:797–808. https://doi.org/10.1038/s41593-019-0375-6.
[21] Folloni D, Verhagen L, Mars RB, Fouragnan E, Constans C, Aubry JF, et al. Manipulation of subcortical and deep cortical activity in the primate brain using transcranial focused ultrasound stimulation. Neuron 2019;101:1109–16. https://doi.org/10.1016/j.neuron.2019.01.019. e5.
[22] Legon W, Bansal P, Ai L, Mueller JK, Meekins G, Gillick B. Safety of transcranial focused ultrasound for human neuromodulation. Preprint at, https://doi.org/10.1101/314856; 2018.
[23] Legon W, Ai L, Bansal P, Mueller JK. Neuromodulation with single-element transcranial focused ultrasound in human thalamus. Hum Brain Mapp 2018;39:1995–2006. https://doi.org/10.1002/hbm.23981.
[24] Legon W, Bansal P, Tyshynsky R, Ai L, Mueller JK. Transcranial focused ultrasound neuromodulation of the human primary motor cortex. Sci Rep 2018;8:10007. https://doi.org/10.1038/s41598-018-28320-1.
[25] Legon W, Sato TF, Opitz A, Mueller J, Barbour A, Williams A, et al. Transcranial focused ultrasound modulates the activity of primary somatosensory cortex in humans. Nat Neurosci 2014;17:322–9. https://doi.org/10.1038/nn.3620.
[26] Lee W, Kim H, Jung Y, Song IU, Chung YA, Yoo SS. Image-guided transcranial focused ultrasound stimulates human primary somatosensory cortex. Sci Rep 2015;5:8743. https://doi.org/10.1038/srep08743.
[27] Lee W, Kim HC, Jung Y, Chung YA, Song IU, Lee JH, et al. Transcranial focused ultrasound stimulation of human primary visual cortex. Sci Rep 2016;6:34026. https://doi.org/10.1038/srep34026. 2016.
[28] Ai L, Bansal P, Mueller JK, Legon W. Effects of transcranial focused ultrasound on human primary motor cortex using 7T fMRI: a pilot study. BMC Neurosci 2018;19:56. https://doi.org/10.1186/s12868-018-0456-6.
[29] Polanía R, Nitsche MA, Ruff CC. Studying and modifying brain function with non-invasive brain stimulation. Nat Neurosci 2018;21:174–87. https://doi.org/10.1038/s41593-017-0054-4.
[30] Guo H, Hamilton II M, Offutt SJ, Gloeckner CD, Li T, Kim Y, et al. Ultrasound produces extensive brain activation via a cochlear pathway. Neuron 2018;98:1020–30. https://doi.org/10.1016/j.neuron.2018.04.036. e4.
[31] Sato T, Shapiro MG, Tsao DY. Ultrasonic neuromodulation causes widespread cortical activation via an indirect auditory mechanism. Neuron 2018;98:1031–41. https://doi.org/10.1016/j.neuron.2018.05.009. e5.
[32] Mohammadjavadi M, Ye PP, Xia A, Brown J, Popelka G, Pauly KB. Elimination of peripheral auditory pathway activation does not affect motor responses from ultrasound neuromodulation. Brain Stimul 2019;12:901–10. https://doi.org/10.1016/j.brs.2019.03.005.
[33] Duecker F, Sack AT. Rethinking the role of sham TMS. Front Psychol 2015;6:210. https://doi.org/10.3389/fpsyg.2015.00210.
[34] Nitsche MA, Cohen LG, Wassermann EM, Priori A, Lang N, Antal A, et al. Transcranial direct current stimulation: state of the art 2008. Brain Stimul 2008;1. https://doi.org/10.1016/j.brs.2008.06.004. 206–23.
[35] Rossi S, Hallett M, Rossini PM, Pascual-Leone A, et al. Safety, ethical considerations, and application guidelines for the use of transcranial magnetic stimulation in clinical practice and research. Clin Neurophysiol 2009;120:2008–39. https://doi.org/10.1016/j.clinph.2009.08.016.
[36] Blackmore J, Shrivastava S, Sallet J, Butler CR, Cleveland RO. Ultrasound neuromodulation; a review of results, mechanisms and safety. Ultrasound Med Biol 2019;45:1509–36. https://doi.org/10.1016/j.ultrasmedbio.2018.12.015.
[37] Rossi S, Hallett M, Rossini PM, Pascual-Leone A. Screening questionnaire before TMS: an update. Clin Neurophysiol 2011;122:1686. https://doi.org/10.1016/j.clinph.2010.12.037.
[38] Huan Y, Parra LC. Fully automated whole-head segmentation with improved smoothness and continuity, with theory reviewed. PLoS One 2015;10:e0125477. https://doi.org/10.1371/journal.pone.0125477.
[39] Treeby BE, Cox BT. k-Wave: MATLAB toolbox for the simulation and reconstruction of photoacoustic wave-fields. J Biomed Optic 2010;15:021314. https://doi.org/10.1117/1.3360308.
[40] Blackmore J, Braun V, Veldsman M, Butler CR, Cleveland RO. Single-element transcranial ultrasound focusing for human neuromodulation. Manuscript submitted for publication; 2019.
[41] Oostenveld R, Fries P, Maris E, Schoffelen J-M. FieldTrip: open source software for advanced analysis of MEG, EEG, and invasive electrophysiological data. Comput Intell Neurosci 2011;2011:156869. https://doi.org/10.1155/2011/156869.
[42] Vaughan HG, Ritter W. The sources of auditory evoked responses recorded from the human scalp. Electroencephalogr Clin Neurophysiol 1970;28:360–7. https://doi.org/10.1016/0013-4694(70)90228-2.
[43] Crowley KE, Colrain IM. A review of the evidence for P2 being an independent component process: age, sleep and modality. Clin. Neuropyshiol. 2004;115:732–44. https://doi.org/10.1016/j.clinph.2003.11.021.
[44] Paiva TO, Almeida PR, Ferreira-Santos F, Vieira JB, Silveira C, Chaves PL, et al. Similar sound intensity dependence of the N1 and P2 components of the auditory ERP: averaged and single trial evidence. Clin Neurophysiol 2016;127:499–508. https://doi.org/10.1016/j.clinph.2015.06.016.
[45] Stenfelt S. Acoustic and physiologic aspects of bone conduction hearing. Adv Otorhinolaryngol 2011;71:10–21. https://doi.org/10.1159/000323574.
[46] Gavrilov LR, Tsirulnikov EM. Focused ultrasound as a tool to input sensory information to humans (Review). Acoust Phys 2012;58:1–21. https://doi.org/10.1134/S1063771012010083.
[47] Stenfelt S, Goode RL. Transmission properties of bone conducted sound: measurements in cadaver heads. J Acoust Soc Am 2005;118:2373–91.
[48] Cai Z, Richards DG, Lenhardt ML, Madsen AG. Response of human skull to bone-conducted sound in the audiometric-ultrasonic range. Int Tinnitus J 2002;8:3–8.
[49] Wattiez N, Constans C, Deffieux T, Daye PM, Tanter M, Aubry JF, et al. Transcranial ultrasonic stimulation modulates single-neuron discharge in

macaques performing an antisaccade task. Brain Stimul 2017;10:1024–31. https://doi.org/10.1016/j.brs.2017.07.007.
[50] Weber DL. Growth of masking and the auditory filter. J Acoust Soc Am 1977;62(2):424–9.
[51] Ter Braack EM, de Vos CC, van Putten MJ. Masking the auditory evoked potential in TMS–EEG: a comparison of various methods. Brain Topogr 2015;28(3):520–8.